Unsteady approach to numerical simulation of conductor motion

Olga A. Ivanova
ivanovaolgaal@mail.ru

Abstract

The mathematical model of unsteady aeroelastic motion of the transmission line conductor is considered. The unsteady approach is developed which is based on the direct numerical simulation of the flow around conductor cross-sections using meshfree lagrangian viscous vortex domains method. To simulate the conductor motion the parallel computer program using MPI technology was developed, which enables to execute computations effectively on various multiprocessor systems. Some test computations were performed. The results were compared with those known from literature.

1 Introduction

An overhead transmission line conductor which is covered by an asymmetric ice deposit can experience galloping — high-amplitude low-frequency wind-induced oscillations. High dynamic loads during galloping can lead to failure of the line hardware, therefore the problem of numerical and experimental modeling of the conductor dynamics is of practical importance [1].

To simulate the conductor galloping only the component of the wind perpendicular to the line is usually taken into account. The aerodynamic loads are usually determined using the flat cross-section method, i.e. the flow around each conductor cross-section is assumed to be plane-parallel and the distributed aerodynamic loads are obtained by interpolation of the loads acting on the cross-sections. Moreover, the aerodynamic loads are usually assumed to be quasi-steady. In this work the unsteady approach is proposed. According to it the aerodynamic loads acting on N separate conductor cross-sections are calculated using some CFD method. In this work meshfree lagrangian viscous vortex domains method [2] is used. Thus a set of N partially independent two-dimensional problems of the flow simulation around the conductor cross-sections must be solved. To reduce the time of computation parallel algorithm based on the MPI technology usage was developed.

2 Governing equations

Let us locate the Cartesian coordinate system as shown on fig. 1; in the equilibrium position without wind action the transmission line is located in the plane Ox_1x_3.

The system of conductor motion equations is based on the equations of motion of the absolutely flexible linearly elastic rod [3]. The terms which take into account the eccentricity of the ice deposit and the equation for the twist angle are added to these

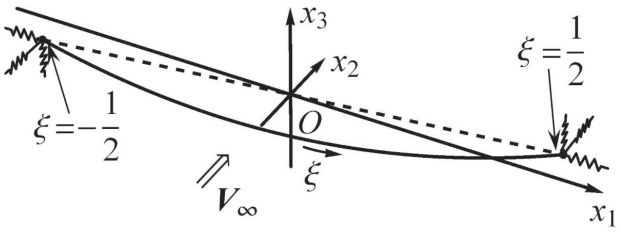

Figure 1: The design diagram

equations. Then the following system is obtained:

$$\left(\frac{Q}{1+Q/EF}x_1'\right)' + C_1 - \ddot{x}_1 = 0, \tag{1}$$

$$\left(\frac{Q}{1+Q/EF}x_2'\right)' + C_2 + \left(1+\frac{Q}{EF}\right)q_2^a - \ddot{x}_2 - h\left(\sin(\theta_s+\theta)\ddot{\theta} + \cos(\theta_s+\theta)\dot{\theta}^2\right) = 0, \tag{2}$$

$$\left(\frac{Q}{1+Q/EF}x_3'\right)' + C_3 + \left(1+\frac{Q}{EF}\right)q_3^a - 1 - \ddot{x}_3 - h\left(\cos(\theta_s+\theta)\ddot{\theta} - \sin(\theta_s+\theta)\dot{\theta}^2\right) = 0, \tag{3}$$

$$\left(x_1'\right)^2 + \left(x_2'\right)^2 + \left(x_3'\right)^2 = \left(1+\frac{Q}{EF}\right)^2, \tag{4}$$

$$GJ\theta'' + C_\theta + M^a - \ddot{\theta} - h\beta\Big(\sin(\theta_s+\theta)\ddot{x}_2 + \cos(\theta_s+\theta)\ddot{x}_3 + \cos(\theta_s+\theta)\Big) = 0. \tag{5}$$

Here dimensionless parameters are: $\xi \in [-1/2, 1/2]$ — natural coordinate on the unstretched conductor, τ — time; $Q(\xi,\tau)$ — tension; $x_i(\xi,\tau)$, $i=1,2,3$ — cartesian coordinates of the conductor axis; $\theta(\xi,\tau)$ — twist angle of the conductor; $C_i(\xi,\tau)$, $C_\theta(\xi,\tau)$ — the functions describing the internal damping forces; $q_k^a(\xi,\tau)$, $k=2,3$, $M^a(\xi,\tau)$ — the aerodynamic loads; $EF=\text{const}$ — axial stiffness; GJ — torsional stiffness; β — parameter characterizing the conductor inertia; $\theta_s(\xi)=\theta_e(\xi)+\theta_G$, $\theta_e(\xi)$ — rotation angle of the unloaded conductor cross-sections. The conductor cross-sections are assumed to be perpendicular to its axis, the axis position in the cross-section is point C. The center of gravity G of the iced conductor cross-section is specified with the distance $h=CG$ and the angle θ_G which is measured at the position corresponding to zero angle of attack as shown on fig. 2. The derivatives with respect to ξ and τ are denoted by the prime and the dot respectively. The units of length, mass and force are the unstretched conductor length $\tilde{L}$, mass and weight respectively; the unit of time is $\sqrt{\tilde{L}/\tilde{g}}$ where $\tilde{g}$ is dimensional gravity acceleration. Hereinafter the tilde accent means that the value is dimensional.

Initial condition for the system (1)–(5) is the equilibrium position in the gravity field $x_{i0}(\xi)$, $i=1,2,3$, $Q_0(\xi)$, $\theta_0(\xi)$.

At the ends ($\xi=\pm 1/2$) the conductor is assumed to be fixed with linear static springs which model the adjacent spans and the insulator strings and have the compliances $S_i^\pm$, $i=1,2,3$:

$$\begin{gathered} x_i(\pm 1/2,\tau) - x_{i0}(\pm 1/2) = S_i^\pm\left(Q\boldsymbol{p}^\pm - Q_0\boldsymbol{p}_0^\pm\right)\Big|_{\xi=\pm 1/2}\cdot\boldsymbol{e}_i, \quad i=1,2,3, \\ \theta(\pm 1/2,\tau) = 0. \end{gathered} \tag{6}$$

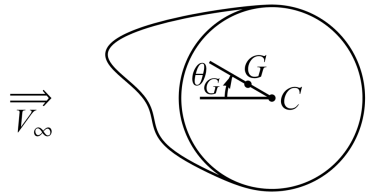

Figure 2: The center of gravity of the conductor cross-section

Here $\boldsymbol{p}^{\pm}$, $\boldsymbol{p}_0^{\pm}$ are unit vectors tangential to the conductor axis at time moments τ and τ_0 respectively (fig. 3).

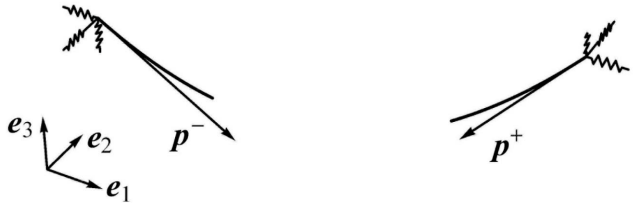

Figure 3: Unit vectors tangential to the conductor axis

The flow around each conductor cross-section is assumed to be plane-parallel so that all the characteristics of the flow don't depend on the x_1 coordinate. The viscous incompressible flow around the airfoil (conductor cross-section) is described by continuity equation

$$\nabla \cdot \boldsymbol{V} = 0$$

and Navier — Stokes equation

$$\frac{\partial \boldsymbol{V}}{\partial t} - \boldsymbol{V} \times \boldsymbol{\Omega} = -\nabla \left(p + \frac{V^2}{2} \right) + \frac{1}{\mathrm{Re}} \nabla^2 \boldsymbol{V},$$

where dimensionless parameters are: $\boldsymbol{V}(x_2, x_3, t)$ — fluid velocity, $\boldsymbol{\Omega} = \nabla \times \boldsymbol{V} = \Omega \boldsymbol{e}_1$ ($\boldsymbol{e}_1$ is axis Ox_1 unit vector) — vorticity, $p(x_2, x_3, t)$ — pressure, Re — Reynolds number. Boundary condition on the airfoil contour is no-slip condition; on infinity all perturbations decay and the flow has uniform velocity $\boldsymbol{V}_\infty$ and pressure p_∞. The aerodynamic loads acting on the airfoil can be determined via the pressure distribution $p(x_2, x_3, t)$.

3 Numerical examples

The conductor motion equations are solved using Galerkin method. The basis functions for the coordinates are the eigenmodes of the conductor small free oscillations and two extra functions needed to correctly satisfy the nonlinear boundary conditions (6). The basis functions for the twist angle θ are trigonometric: $\sqrt{2} \sin \pi k(\xi + 1/2)$, $k = 1, 2, \ldots$ Using Galerkin method the system of partial differential equations (1)–(5) is reduced to the system of ordinary differential and algebraic equations. The functions $C_j(\xi, \tau)$, $j = 1, 2, 3$, $C_\theta(\xi, \tau)$ which describe the internal damping forces are taken in the form of modal damping.

The flow around each cross-section of the conductor is simulated using meshfree viscous vortex domains method [2] with the modified numerical scheme [4].

The following parallel computer algorithm based on MPI technology usage is proposed to simulate the unsteady aeroelastic conductor motion. The aerodynamic loads are calculated at N equally-spaced conductor cross-sections; the flow around each cross-section is simulated by a group of m processors. Each group has a local main processor (LMP); the main processor of the first group is also the main processor (MP) of the whole task. At each time step the following operations are executed.

1. Each group solves two-dimensional problem of the flow around one cross-section during 1 time step (fig. 4).

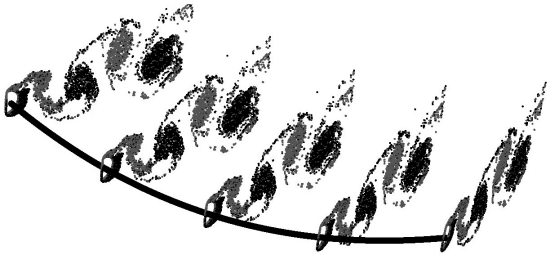

Figure 4: Flat cross-section method llustration

2. LMP's calculate the aerodynamic loads on the cross-sections and send calculated values to MP.

3. MP interpolates aerodynamic loads acting on the cross-sections to obtain $q_2^a(\xi,\tau)$, $q_3^a(\xi,\tau)$, $M^a(\xi,\tau)$ and solves the nonlinear system obtained by Galerkin method during 1 time step.

4. MP broadcasts x_k, θ and their time derivatives to all processes.

5. All processes calculate the positions and angles of the cross-sections on the next time step.

On the base of the proposed algorithm the parallel computer program PROVOD is developed. It allows also to perform quasi-steady computation, i.e. to use the stationary aerodynamic drag C_{xa}, lift C_{ya} and moment C_m coefficients of the cross-sections instead of simulation of the flow around them.

The development of periodic high-amplitude galloping motion sometimes takes considerable time (up to hundreds of seconds). To reduce the time of computation it is proposed to execute quasi-steady simulation until the periodic trajectory is reached and then to change the way of the loads calculation and to execute the unsteady simulation using viscous vortex domains method.

3.1 Quasi-steady simulation: dead ended conductor

The simulation of galloping of the dead ended conductor ($S_1^{\pm} = S_2^{\pm} = S_3^{\pm} = 0$) described in [5, 6] was performed; the dimensionless parameters of the conductor were: axial stiffness $EF = 12\,254$, torsional stiffness $GJ = 800.6$,, horizontal component of tension $Q_0(0) = 7.42$, $h = 1.37 \cdot 10^{-5}$, $\beta = 1.66 \cdot 10^8$, sag-to-span ratio $w = -x_{30}(0) = 0.0168$. As it is not clear from [6] how the initial rotation angle θ_e was introduced it was assumed to be $\theta_e = 170°$.

The conductor cross-section and its stationary aerodynamic coefficients are shown on fig. 5. The analysis of the stationary aerodynamic coefficients shows that Den-Hartog aerodynamic instability condition [7]

$$C_{xa}(\alpha) + C'_{ya}(\alpha) < 0$$

is satisfied for the angles of attack $\alpha \in [30°; 52°]$ и $\alpha \in [167°; 202°]$.

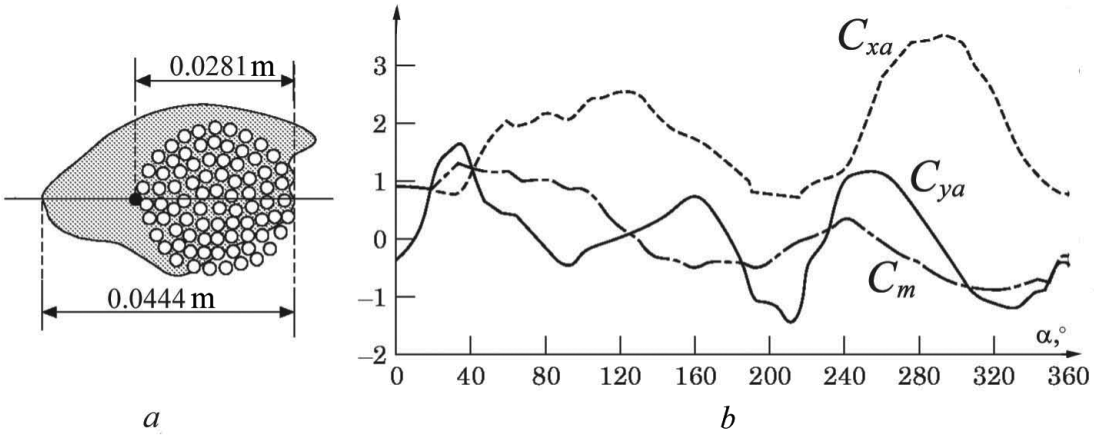

Figure 5: The airfoil (a) and its stationary aerodynamic coefficients (b) [5, 6]

The trajectory of the central point on the conductor ($\xi = 0$) is shown on fig. 6. One eigenmode of small free conductor oscillations in each direction was used in the simulation. Test computations have shown that the increase of the number of basis functions doesn't lead to the perceptible change of galloping characteristics.

As follows from fig. 6, the peak-to-peak amplitude of vertical movement is 1.1 m. This is in good agreement with the result of simulation [6]. The trajectory of central point of the conductor has the U-shaped form as in [6]. This phenomenon can be explained by the fact that the ratio of the first eigenfrequencies of vertical (in the Ox_1x_3-plane) and transverse (in the direction of Ox_2 axis) — 0.70 Hz to 0.38 Hz — is close to 2.

3.2 Quasi-steady simulation: conductor with elastically fixed ends

The galloping motion observed for the central span of the three-span test line is described in [8]. The central span was covered by an artificial U-shaped "icing" (fig. 7). This case of galloping was reproduced numerically in [9, 5] assuming that the aerodynamic loads were quasi-steady.

The conductor cross-section and its stationary aerodynamic coefficients are shown on fig. 7. The analysis of the stationary aerodynamic coefficients has shown that Den-Hartog aerodynamic instability condition is satisfied for the angles of attack $\alpha \in [17°; 90°]$, $\alpha \in [152°; 204°]$, $\alpha \in [261°; 327°]$.

Dimensional parameters of the line are given in [9, 10]. Dimensionless parameters are the following: axial stiffness $EF = 6909$, torsional stiffness $GJ = 742.5$, $h = 6.5 \cdot 10^{-6}$, $\beta = 6.3 \cdot 10^8$, horizontal component of tension $Q_0(0) = 7.44$, sag-to-span ratio $w = 0.0168$. The initial rotation angle was $\theta_e = 141°$, so under the action of the gravity force the central cross-section equilibrium orientation angle became $\theta_s(0) \approx 180°$.

The dimensionless strings' compliances $S_1^{\pm}$, $S_2^{\pm}$ were chosen so that the first natural frequencies of the central span with elastically fixed ends were equal to the corresponding natural frequencies of the full three-span line (0.29 Hz in the Ox_1x_3-plane and 0.24 Hz in the Ox_2 direction): $S_1^{\pm} = 0.00073$, $S_2^{\pm} = 0.0095$.

Numerical simulation of galloping of the central span has shown that peak-to-peak amplitude of vertical motion was about 2.3 m. Vertical and angular displacements of the central point of the span from its equilibrium position are shown on fig. 8. The results of this research are in good agreement with the results of numerical simulation [9] and in satisfactory agreement with experiment [8].

One eigenmode of small free conductor oscillations in each direction was used in the simulation. Test computations have shown that the increase of the number of basis functions doesn't lead to the perceptible change of galloping characteristics.

3.3 Unsteady conductor motion simulation

The unsteady motion of the conductor with the cross-section considered in [11, 12] (fig. 9, a) was simulated using the algorithm proposed in this work. Dimensionless parameters were the following: axial stiffness $EF = 6909$, torsional stiffness $GJ = 334.8$, $h = 6.2 \cdot 10^{-6}$, $\beta = 4.3 \cdot 10^8$, horizontal component of tension $Q_0(0) = 7.44$, sag-to-span ratio $w = 0.0168$. The initial cross-section orientation angle was $\theta_e = -46^\circ$ which under the action of the gravity force resulted in the central cross-section equilibrium orientation angle close to $\theta_s(0) \approx 7^\circ$. The end springs compliances were $S_1^{\pm} = 0.00096$, $S_2^{\pm} = 0.0085$, $S_3^{\pm} = 0$. The basis contained one eigenmode of small free oscillations in each direction.

Preliminarily the stationary aerodynamic coefficients C_{xa}, C_{ya}, C_m of this airfoil were obtained via time averaging of the corresponding unstationary coefficients over 7 000 time steps (fig. 9, b). The simulation parameters were the following: vortex element radius $\varepsilon = 0.008$, collapse radius $\varepsilon_{col} = 0.002$, incoming flow velocity $V_\infty = 1$, time step $\Delta\tau = 0.004$, Reynolds number $\mathrm{Re} = 1000$. The airfoil was modeled by 245 panels. The analysis of the dependencies $C_{xa}(\alpha)$, $C_{ya}(\alpha)$, $C_m(\alpha)$ approximated by smooth curves has shown that the

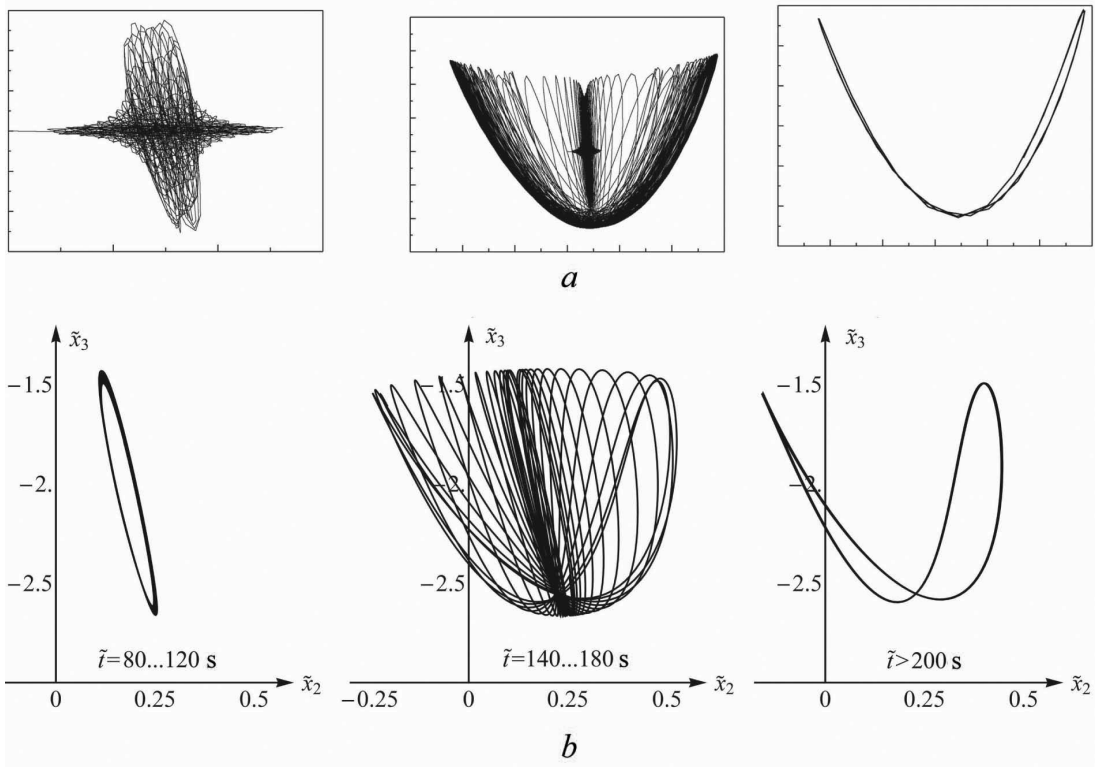

Figure 6: The development of galloping: the results of simulation [6] (a), the results of this research (b)

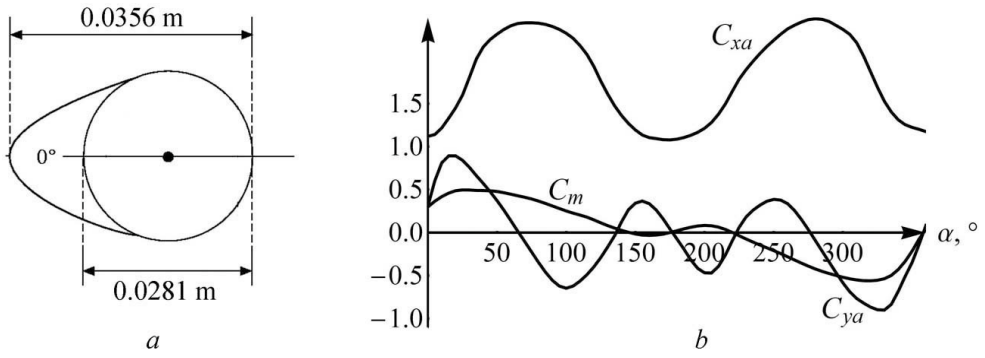

Figure 7: U-shaped airfoil [8] (a) and its stationary aerodynamic coefficients [5] (b)

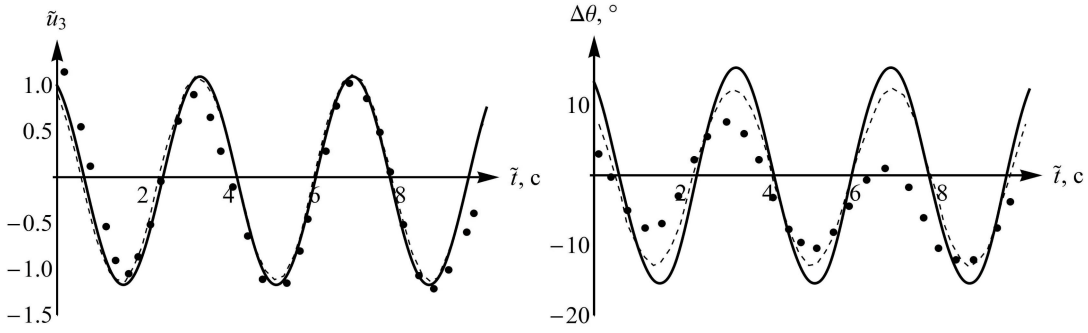

Figure 8: Vertical $\tilde{u}_3$ and angular $\Delta\theta$ displacements of the central point of the span versus time: points — experiment [8], dashed line — simulation [9], solid line — this work

Den-Hartog instability condition is satisfied in the interval $\alpha \in [-7°; 11°]$.

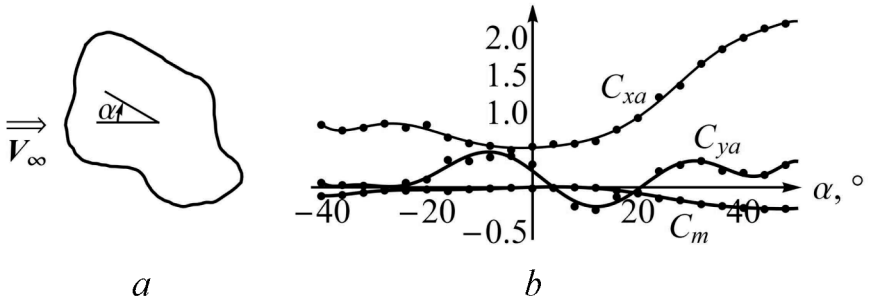

Figure 9: Stationary aerodynamic coefficients $C_{xa}(\alpha)$, $C_{ya}(\alpha)$, $C_m(\alpha)$ of the iced cross-section (a) approximated by smooth functions (b)

At first stage the quasi-steady loads were used in the computation until time moment $\tilde{t}^* = 180$ s; on the next stage the unsteady loads on the conductor cross-sections were determined using viscous vortex domains method. The number of conductor cross-sections considered was equal to $N = 16$; the flow around each of them was simulated in the parallel mode by $m = 8$ processors. Hereby the unsteady calculation required the usage of 128 computing cores of the cluster MVS-100K (Joint Supercomputer Center of the Russian Academy of Sciences) and took about 140 hours. The acceleration of the parallel computation in comparison with the computation in sequential mode was close to 65 times.

Vertical coordinate $\tilde{x}_3(0)$ and angular position $\theta(0)$ of the central point of the conductor are shown on fig. 10. It can be observed that the galloping amplitude obtained in the

unsteady simulation is 12 % less in comparison with the quasi-steady simulation and is finally about 0.65 m. The amplitude of rotational oscillations doesn't change significantly and is approximately 9°. It can be noticed that the conductor natural high-frequency rotational oscillations are superimposed on the rotational motion coherent with the vertical one.

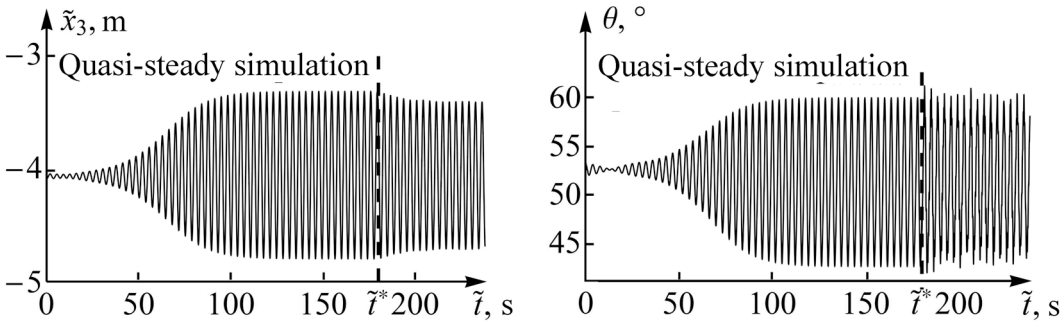

Figure 10: Vertical coordinate $\tilde{x}_3$ and rotation angle θ of the central point on the conductor versus time

4 Conclusion and future work

The algorithm of simulation of the unsteady aeroelastic oscillations of transmission line conductor with asymmetrical cross-section was proposed and the parallel computer program PROVOD based on this algorithm was developed. The program allows also to determine stationary aerodynamic coefficients of the airfoil and to perform quasi-steady simulations. To simulate the flow around conductor cross-sections and to calculate the unsteady aerodynamic loads acting on them meshfree viscous vortex domains method is used. The results of test computations are in good qualitative and quantitative agreement with known experimental and numerical results. The developed algorithm and program can be used to investigate unsteady aeroelastic oscillations of rods and cables. The results of this work can be further developed to simulate the flow-induced oscillations of more complicated constructions such as bundled conductors and heat exchanger tube bundles.

Acknowledgements

The work was supported by Ministry of education and science of Russia (project MK-3705.2014.8). The author thanks Joint Supercomputer Center of the Russian Academy of Sciences for the given possibility of supercomputer MVS-100k usage.

References

[1] EPRI. Transmission line reference book: wind-induced conductor motion. Palo Alto (California): Electrical Power Research Institute, 1979.

[2] Dynnikova G.Ya. The Viscous Vortex Domains (VVD) method for non-stationary viscous incompressible flow simulation. The IV European Conference on Computational Mechanics: book of proceedings. Paris (France), 2010.

[3] Svetlicky V.A. Dynamics of rods. Springer, 2005.

[4] Marchevsky I.K., Moreva V.S. On modified numerical schemes in vortex element method for 2d flow simulation around airfoils. World Academy of Science, Engineering and Technology, 2012. V. 68. P. 1594–1600.

[5] Desai Y.M., Yu P., Shah A.H., Popplewell N. Perturbation-based finite element analyses of transmission line galloping. Journal of Sound and Vibration, 1996. V. 191, N 4. P. 469–489.

[6] Liu X., Yan B., Zhang H., Zhou S. Nonlinear numerical simulation method for galloping of iced conductor. Applied Mathematics and Mechanics (English Edition), 2009. V. 30, N 4. P. 489–501.

[7] Den Hartog J.P. Transmission line vibration due to sleet. AIEE Transactions, 1932. V. 51. P. 1074–1076.

[8] Chan J.K. Modelling of single conductor galloping. Canadian Electrical Association Report 321-T-672A. Montreal, 1992.

[9] Keutgen R. Galloping phenomena: a finite element approach: Ph.D. Thesis. Liege (Belgium), 1998.

[10] Wang X., Lou W.-J. Numerical approach to galloping of conductor. The 7th Asia-Pacific Conference on Wind Engineering: book of proceedings. Taipei (Taiwan), 2009.

[11] Lukjanova V.N. The development of the methods of analysis of absolutely flexible rods (conductors) during icing and unsteady oscillations. Ph.D. Thesis. Moscow (Russia), 1987. [in Russian]

[12] Marchevsky I.K. Mathematical modeling of the flow around an airfoil and its Lyapunov stability investigation: Ph.D. Thesis. Moscow (Russia), 2008. [in Russian]

Olga A. Ivanova, Moscow, Russia